Title

A coupled in vitro/in vivo approach for engineering a heterologous type III PKS to enhance polyketide biosynthesis in Saccharomyces cerevisiae.

Journal

Biotechnology and Bioengineering, 115(6)

Authors

Vickery, Christopher
Cardenas, Javier
Bowman, Marianne
et al.

Publication Date

2018-06-01

DOI

10.1002/bit.26564

Peer reviewed

Published in final edited form as:

Biotechnol Bioeng. 2018 June ; 115(6): 1394–1402. doi:10.1002/bit.26564.

A coupled *in vitro/in vivo* approach for engineering a heterologous Type III PKS to enhance polyketide biosynthesis in *Saccharomyces cerevisiae*

Christopher R. Vickery[a,c,+], **Javier Cardenas**[b,+], **Marianne Bowman**[a], **Michael D. Burkart**[c], **Nancy A. Da Silva**[b,*], **Joseph P. Noel**[a,*]

[a]Howard Hughes Medical Institute, Jack H. Skirball Center for Chemical Biology and Proteomics, The Salk Institute for Biological Studies, La Jolla, CA, 92037 USA

[b]Department of Chemical Engineering and Materials Science, University of California, Irvine, CA, 92697-2575 USA

[c]Department of Chemistry and Biochemistry, University of California, San Diego, La Jolla, CA 92093

Abstract

Polyketides are attractive compounds for uses ranging from biorenewable chemical precursors to high-value therapeutics. In many cases, synthesis in a heterologous host is required to produce these compounds in industrially relevant quantities. The type III polyketide synthase 2-pyrone synthase (2-PS) from *Gerbera hybrida* was used for the production of triacetic acid lactone (TAL) in *Saccharomyces cerevisiae*. Initial *in vitro* characterization of 2-PS led to the identification of active site variants with improved kinetic properties relative to wildtype. Further *in vivo* evaluation in *S. cerevisiae* suggested certain 2-PS mutations altered enzyme stability during fermentation. *In vivo* experiments also revealed beneficial cysteine to serine mutations that were not initially explored due to their distance from the active site of 2-PS, leading to the design of additional 2-PS enzymes. While these variants showed varying catalytic efficiencies *in vitro*, they exhibited up to 2.5-fold increases in TAL production when expressed in *S. cerevisiae*. Coupling of the 2-PS variant [C35S,C372S] to an engineered *S. cerevisiae* strain led to over 10 g/L TAL at 38% of theoretical yield following fed-batch fermentation, the highest reported. Our studies demonstrate the success of a coupled *in vitro/in vivo* approach to engineering enzymes and provide insight on cysteine-rich enzymes and design principles towards their use in non-native microbial hosts.

Keywords

2-pyrone synthase; triacetic acid lactone; polyketide; *Saccharomyces cerevisiae*; enzyme engineering

[*]Corresponding authors: **Tel:** (+1) 949-824-8288, **Fax:** (+1) 949-824-2541, ndasilva@uci.edu, **Tel:** (+1) 858-453-4100 ext. 1442, **Fax:** (+1) 858-597-0855, noel@salk.edu.

[+]Equal contribution

7.Conflicts of interest

The authors claim no conflicts of interest related to the publication of this manuscript.

1. Introduction

With growing interest in bio-based products, the demand for novel semisynthetic and biosynthetic routes toward unique compounds is ever increasing. These natural products are often produced industrially in production organisms equipped with heterologous enzymes (Nevoigt, 2008). This is due to the need to leverage well-known, valuable industrial strains in producing non-native molecules and the potential to produce intermediates and analogs by directed biosynthesis. Plant-derived polyketides have gained acceptance as commercially valuable compounds for production in microorganisms, as this class of molecules possesses a wide range of structural diversity and bioactive properties (Marienhagen and Bott, 2013; Vickery et al., 2016).

Type III polyketide synthases (T3PKSs) are enzymes that produce polyketides in plants (Stewart et al., 2013). These homo-dimeric enzymes utilize a variety of acyl-CoA substrates to produce a plethora of natural products with varying structures and properties *via* iterative decarboxylative condensation reactions followed by cyclization (Hertweck, 2009). Recently, there has been great interest in utilizing these synthases for the production of chemically diverse and industrially relevant molecules (Stewart et al., 2013). The relatively small size (~43 kDa) and ability to act without additional cofactors or protein partners makes this enzyme class ideal for heterologous production of polyketide products (Pfeifer and Khosla, 2001). In addition to the products produced naturally by Type III PKSs, they can be leveraged to produce new molecular scaffolds and compound classes. Small changes in the active site can modulate the chemistry of product formation, leading to altered polyketide scaffolds (Austin et al., 2004; Jez et al., 2001). *In vitro* supplementation of different CoA substrates leads to the formation of new and unnatural polyketide products (Jez et al., 2002; Kim et al., 2009; Wang et al., 2016). The potential of type III PKSs to produce both useful natural products and new valuable molecules makes them highly attractive for large scale biosynthesis using heterologous hosts.

The polyketide synthase 2-PS is responsible for making the pyrone precursor triacetic acid lactone (TAL) of the *G. hybrida* natural products gerberin and parasorboside (Eckermann et al., 1998). Biosynthesis of TAL requires the condensation of two malonyl CoA molecules with one acetyl CoA starter unit, followed by cyclization and aromatization (Figure 1), and this reaction has previously been monitored *in vitro* (Jez et al., 2000a). Previous work has demonstrated the microbial synthesis of TAL via 2-PS (Cardenas and Da Silva, 2014; Cardenas and Da Silva, 2016; Chia et al., 2012; Saunders et al., 2015; Tang et al., 2013; Xie et al., 2006). Tang and coworkers employed a random mutagenesis approach to obtain improved 2-PS enzymes (Tang et al., 2013). These mutants exhibited mutations in and around the active site and led to greater production of TAL in *Escherichia coli* due to increased catalytic activity. The promise of TAL as a biologically-derived intermediate for subsequent conversion to various chemicals has also been demonstrated (Chia et al., 2012; Kraus et al., 2016; Schwartz et al., 2014; Shanks and Keeling, 2017; Xie et al., 2006).

In the current study, rational enzyme engineering was performed using the *G. hybrida* 2-PS to increase TAL production in *S. cerevisiae*. An advantage of this yeast is the minimal toxicity of the TAL product (Cardenas and Da Silva, 2014). Structure-based site-directed

mutagenesis led to the testing of 41 variants *in vivo*. Variants possessed amino acid changes both in and around the active site, as well as modification of surface cysteines to increase both catalytic efficiency and *in vivo* stability. These results were coupled with *in vitro* enzymatic characterization of several variants to uncover enzyme properties conferring increased production of TAL. This novel approach of coupling *in vitro* with *in vivo* analysis facilitated the creation of a useful and stable enzyme as applied in a biological fermentation process. These data provide valuable information for designing heterologous synthase systems for improved catalytic efficiency and stability in microbial systems, as demonstrated for *S. cerevisiae* in this work. The success of such a strategy was further validated by fed-batch cultivation of an engineered yeast strain expressing a variant 2-PS and demonstrating increased performance through improved titers and yields. This coupled *in vitro/in vivo* engineering approach and the insights provided should be valuable for improving biosynthesis of other natural products.

2. Materials and Methods

2.1 Strains and plasmids

E. coli strain XL1-Blue (Stratagene, Santa Clara, CA) was used for amplification of yeast shuttle vectors, and strain BL21 (DE3) (EMD Millipore, Billerica, MA) for expression of 2-PS and its variants. The Quikchange protocol (Qiagen, Valencia, CA) was used to construct all mutants of 2-PS in a pHIS8 vector background from the vector used by Jez et. al. (Jez et al., 2000a) *Saccharomyces cerevisiae* strain BJ5464 (*MATα ura3–52 trp1 leu2Δ1 his3Δ200 pep4::HIS3 prb1Δ1.6R can1 GAL)* ((Jones, 1991)) was used as the base strain for TAL production. The engineered strain BJΔ*pyc2*Δ*nte1* (BJ5464 *pyc2::TRP1 nte1::LEU2*) (Cardenas and Da Silva, 2014) was used for fed-batch bioreactor studies. Strains BYt (BY4741Δ*trp1*), BYtΔ*prb1*, and BYtΔ*pep4*Δ*prb1* (Cardenas and Da Silva, 2014) were used to evaluate the effects of the protease knockouts.

Restriction enzymes, T4 DNA ligase, Taq DNA polymerase, and deoxynucleotides were purchased from New England Biolabs (Ipswich, MA). Oligonucleotide primers were purchased from IDT DNA (San Diego, CA). The *Gerbera hybrida g2ps1* gene encoding the 2-PS and all variants (Supplementary Table 1) were PCR amplified from the pHIS8 cassette (Jez et al., 2000a) using KOD Hot-start polymerase (EMD Chemicals, San Diego, CA). Following *SpeI* and *XhoI* digestion, the gene was inserted into pXP842 (Shen et al., 2012) using the Rapid DNA Ligation Kit (Thermo Scientific, Waltham, MA). This 2μ-based vector carries the glucose-repressed *S. cerevisiae ADH2* promoter, *CYC1* terminator, and a loxP-flanked *URA3* selection marker. With this promoter, TAL production occurs during the ethanol phase following glucose depletion. Plasmid recovery was performed using the GeneJet™ Plasmid Miniprep Kit (Thermo Scientific, Waltham, MA) and DNA sequence analysis confirmed the correct sequence of all PCR-amplified inserts (GeneWiz, South Plainfield, NJ; Eton Biosciences, San Diego, CA).Yeast cells were transformed as previously described (Gietz et al., 1992; Hill et al., 1991).

2.2 Media and cultivation

Luria-Bertani (LB) media was used for proliferation of XL1-Blue cells with 150 mg/L ampicillin for selection of plasmid-containing strains (Sambrook and Russell, 2001). Terrific broth (TB) media was used for the production of 2-PS enzyme encoded in the pHIS8 vector background. For the inoculum cultures, *S. cerevisiae* strains were grown for 16 h overnight in 5 mL selective SDC(A) medium (1% dextrose, 0.67% yeast nitrogen base, 0.5% Bacto casamino acids, 0.5% ammonium sulfate and 100 mg/L adenine) in an air shaker (New Brunswick Scientific) at 250 rpm and 30°C, and used to inoculate flask cultures to an initial cell density (OD_{600}) of 0.3 (Shimadzu UV-2450 UV-VIS Spectrophotometer, Columbia, MD). Complex YPD medium (1% dextrose; 1% Bacto yeast extract; 2 % Bacto peptone) was used for the flask cultivations and a sample was taken at 48 h. Cell densities were determined and the samples were centrifuged at 3,000 rpm (2,600 g) for 5 min at 4°C (Beckman GS-6R Centrifuge, Brea, CA). The supernatants were stored at 4°C for HPLC analysis of TAL levels in the culture broth.

2.3 *In vitro* enzyme assays

In vitro assessment of 2-PS activity was carried out as previously described (Jez et al., 2000a) in a reaction containing 100 mM sodium phosphate buffer pH 7.0, 60 μM malonyl CoA, and varying concentrations of acetyl CoA. However, after quenching with 5% acetic acid, reactions were directly analyzed on a Shimadzu LCMS-2020 UPLC-MS using a Phenomenex Kinetex C18 reverse phase column. Samples were monitored on the negative ion channel at 125.11 m/z, and the area under the mass peak was used to quantify TAL.

Linear activity for each mutant was assessed as previously described (Jez et al., 2000a). For each mutant, a suitable reaction time was determined (6 to 15 minutes), and 0.25—1 μg enzyme was incubated with saturating malonyl CoA concentrations and concentrations ranging from 250 nM to 32 μM acetyl CoA or 125 nM to 16 μM acetyl CoA for the determined length of time and quenched with 5% acetic acid. Integration of the SIM mass spectrum in negative mode measuring for a mass of 125.11 was quantified by comparison to a standard curve of TAL consisting of concentrations ranging from 50 nM to 1 μM. Reactions were performed in triplicate and analyzed using the Michaelis-Menten equation in GraphPad Prism 5 to obtain kinetic parameters.

Melting temperature studies were performed using a Roche LightCycler 480 in white 384 well plates (Roche, Basel, Switzerland). In a 20 μL well, 2-PS mutants were incubated in enzyme reaction buffer at 15 μM and 10x Sypro Orange dye (Roche, Basel, Switzerland). The temperature was increased by 0.02°C/sec and fluorescence was measured at an excitation wavelength of 465 nm and emission at 570 nm. Raw data were processed by plotting the first derivative to identify the inflection point, and the temperature at which this inflection point occurred was used at the T_m.

Half-life determination for wildtype and 5 mutants was assayed by incubation of the enzyme at room temperature in 100 mM Sodium phosphate buffer pH 7.0 for intervals of time from 0 minutes to 180 minutes. Every 10 minutes for the first hour and then every 30 minutes after that, an activity assay was performed. Assays were performed as described above,

except that only 64 μM malonyl CoA was added, and all reactions were incubated for 6 minutes before quenching and TAL measurement. The resulting activity was plotted and analyzed using a single decay equation to obtain the half-life of each mutant.

Oxidation studies were performed following cultivation of *S. cerevisiae* using a standard DTNB assay. The reaction consisted of 150 mM tris buffer (pH 8.0), 4mM DTNB, and 2 nmol of purified protein extract. Extracts were performed at 24 h, 36 h, and 48 h during both aerobic and anaerobic yeast culture. Using a modified purification scheme as done previously (Jez et al., 2000b), additional protection of purified protein was achieved via nitrogen-sparging prior to the assay. The free thiol levels were reported using DTT standards from 0–20 μM and detecting absorbance at 312 nm (Shimadzu UV-2450 spectrophotometer; Columbia, MD).

2.4 HPLC quantification of TAL in yeast culture broth

The concentration of triacetic acid lactone was measured by HPLC using a Shimadzu HPLC system: LC-10AT pumps (Shimadzu), UV-VIS detector (SPD-10A VP, Shimadzu), Zorbax SB-C18 reversed-phase column (2.1×150 mm, Agilent Technologies). Acetonitrile buffered in 1% acetic acid was used as the mobile phase, while HPLC grade water buffered in 1% acetic acid was used as the aqueous phase. A gradient program using a 95–85% Pump B gradient (H_2O with 1% acetic acid) provided an elution time of approximately 12 minutes (flow rate 0.25 mL/min, column temperature 25°C).

2.5 Fed-batch cultivation

A New Brunswick BioFlo III system with a 2.5 L vessel was employed to maintain cultivation parameters during fed-batch operation. An initial 5mL SDC(A) culture of the engineered strain was used to inoculate a 50 mL YPD shake flask culture for use as the seed inoculum for the bioreactor. Following inoculation to an OD_{600} of 0.3, the fermenter pH was controlled at pH 6 by automatic supply of either 6 M sodium hydroxide or hydrochloric acid. YPD medium was used for this initial batch phase. Antifoam SE-15 (Sigma) was added as needed, controlled using the antifoam probe. Dissolved oxygen (DO) was maintained at 20% by using a 400 rpm agitation speed and supplying sparged air at an initial rate of 0.2 vvm. While agitation was kept constant, the aeration rate was allowed to increase in order to ensure DO levels could be maintained, and no additional control was employed for this batch mode operation. The cultivation proceeded under these conditions for 12 h before the carbon source feed was initiated at 1.5 mL/h (glucose feed, 3.6 M). Nitrogen-containing amino acids were supplied with the glucose feed in order to support a 35:1 (g/g) carbon-to-nitrogen ratio, ideal for high fermentative capacity (Albers et al., 1996; Manikandan et al., 2010), as follows: 869 mg/L L-arginine, 960 mg/L L-aspartic acid, 12.4 mg/L L-glutamine, 360 mg/L L-glutamic acid, 84.5 mg/L L-lysine-HCl, 100 mg/L adenine sulfate. The glucose feed rate was varied to maintain DO levels at 20% with constant agitation (400 rpm) and aeration (0.8 vvm).

3. Results

3.1 *In vitro* activity of 2-PS and 2-PS variants

Following expression and purification from *E. coli*, recombinant wildtype 2-PS produced TAL when incubated with the precursors acetyl-CoA and malonyl-CoA (Figure 1). TAL formation was also observed when 2-PS was incubated only with malonyl-CoA, due to the ability of 2-PS to catalyze decarboxylation of malonyl-CoA to form acetyl-CoA (Eckermann et al., 1998). Kinetic analysis was performed with varying concentrations of acetyl-CoA and a fixed concentration of malonyl-CoA as previously described (Jez et al., 2000a). Although some background activity was present in all reactions due to the decarboxylation event, TAL formation was greater in the presence of acetyl-CoA (Supplementary Figure 1). 2-PS was measured to have a K_m of 1.0 ± 0.2 μM, a k_{cat} of 0.54 ± 0.02 m^{-1}, and k_{cat}/K_m of 8900 M^{-1} s^{-1} with respect to acetyl-CoA, similar to previously reported values (Jez et al., 2000a).

Initial *in vitro* kinetic analysis of 2-PS variants was performed on enzymes expressed and purified from *E. coli* (Table 1). Amino acid variants of 2-PS were devised by investigating the crystal structure of 2-PS (PDBid 1EE0) (Jez et al., 2000a). Alteration of the active site of Type III PKSs can influence the kinetics of product formation (Jez et al., 2002). Therefore, we analyzed the active site of 2-PS and identified residues that, when mutated to larger hydrophobic amino acids, would restrict the active site size and increase production of TAL (Supplementary Figure 2). We also noted that in the structure of 2-PS, C35 was positioned very close to C35 of another enzyme monomer. Mutation of C35 to serine would help avoid unfavorable disulfide bond formation (Costa et al., 2007). A C35S mutation increased TAL titer levels, and thus it was coupled with our selected active site mutations. Of the 12 mutants chosen for evaluation, eight produced sufficient quantities of soluble protein for kinetic analysis (Supplementary Figure 3A). The [C35SL202F] variant displayed the greatest catalytic efficiency with a k_{cat}/K_m of 18000 $M^{-1}s^{-1}$ (Table 1, Supplementary Figure 3B). Both [C35S] and [C35S,C372S] mutants displayed elevated catalytic efficiency over wildtype. Mutants with decreased catalytic efficiencies included [C35A], [C35S,I343F], [C35S,L268F], [L268F], and [C35S,I201M].

3.2 *In vivo* evaluation of 2-PS variants

To compare *in vivo* TAL biosynthesis levels, the 2-PS variants were inserted into a 2μ-based vector under the control of the *ADH2* promoter and transformed into *S. cerevisiae* strain BJ5464. An increase in TAL titer of up to 2-fold was observed for the 2-PS variants relative to that for the wildtype 2-PS (0.48 g/L) (Figure 2). Notably, [C35S], [C35S,L202M], [C35S,L202F], and [C35S,L268M] showed comparable increases in TAL titer to ~0.85 g/L TAL. [C35S,L268F] and [C35S,T137F] both increased titer 2.2-fold to ~1.1 g/L TAL. [C35A], [L268F], [C35S,I343F], and [C35S,I201M] had a negative impact on TAL titers.

3.3 Changing external cysteines to improve 2-PS variants

Due to the success of the C35S 2-PS mutant, all cysteine residues found in 2-PS, excluding the conserved C169 residue of the conserved Cys-His-Asn catalytic triad (Austin and Noel, 2003), were modified to either alanine or serine. Based on the 2-PS crystal structure, cysteines C35, C372, and C89 are exposed on the surface, while C65, C135, C195, and

C346 are buried in the protein structure. When combined with a C35 S mutation, substitution with serine resulted in significantly greater *in vivo* TAL production than an alanine mutation for each cysteine except for C195 and C346, potentially due to their location within the hydrophobic protein core (Figure 3). Position 135 has the potential to interact closely with C195 *via* a disulfide bond, but changing either residue did not severely reduce TAL production. Variants [C35S, C65S], [C35S, C89S], [C35S, C135S], and [C35S, C372S] all performed significantly better than both wildtype and [C35S] resulting in >1 g/L TAL.

To further investigate the potential of enzyme stability *via* cysteine exchange, cysteine to serine mutations were introduced to either the wildtype 2-PS enzyme or the [C35S] variant, generating a collection of mixed cysteine mutants across all cysteines in the enzyme (Figure 4). Cysteine variants that did not contain a C35S mutation exhibited a decrease in *in vivo* TAL production, except [C89S,C372S] that produced TAL levels similar to C35S. However, the same cysteine mutations performed on the [C35S] enzyme consistently led to a ~2-fold increase in TAL production relative to the wildtype, although only small increases beyond that observed for the [C35S] mutation alone. The one exception and best performer, [C35S,C372S], produced 1.2 g/L TAL *in vivo*, 2.5-fold higher than the native 2-PS. Kinetic analysis revealed a k_{cat}/K_m of 1.2 $\times 10^4$ $M^{-1}s^{-1}$, approximately 1.5-fold greater than wildtype 2-PS.

3.4 Investigating biophysical properties of 2-PS variants

In order to assess the *in vitro* stability of 2-PS variants, they were subjected to thermal stability analysis by thermal denaturation (Niesen et al., 2007) (Supplementary Figure 4). Wildtype 2-PS possessed a melting temperature (T_m) of 60.7°C. Only one variant, [C35SI201M], possessed a greater T_m than wildtype, at 61.8°C. In general, cysteine mutations did not greatly alter the T_m of enzyme variants. However, mutations in the active site decreased the T_m, ranging from 41.1°C to 55°C.

Five representative mutant enzymes were selected to determine *in vitro* stability of 2-PS over increasing periods of time. Variants were incubated at room temperature in reaction buffer and assayed at several time points, beginning at the initial time of incubation (Figure 5A). The [C35S] and [C35S,C372S] variants displayed increasing half-life values, while [C35A] showed a decrease in half-life. [L268F] exhibited a greater half-life than WT and a comparable half-life to [C35S], and the [C35S,L202F] variant possessed the greatest half-life of nearly 100 minutes.

To further understand possible effects of surface modifications on the biological and cellular processes, a rapid free thiol detection assay with 5,5'-dithiobis-2-nitrobenzoic acid (DNTB) was used. This assay was performed on wildtype 2-PS purified from *S. cerevisiae* following 24 h, 36 h, and 48 h cultivation. Both aerobic and anaerobic growth were investigated (Figure 5B); in both cases, a sharp decrease in free thiol levels was observed after 36 h. Free thiol levels were significantly less at all time points during anaerobic cultivation.

In order to assess the effects of certain mutants on expression levels in yeast, representative variants were screened by Western blot (Supplementary Figure 5). Interestingly, all variants

displayed roughly equal protein levels except for [C35A] and [C35S,C372S]. The low *in vivo* levels of C35A easily explain the sharp drop in TAL production, while the relatively high levels of [C35S,C372S] possibly account for the greater TAL titers.

3.5 Effects of protease knockouts on TAL synthesis in yeast

To test the direct impact proteases have on 2-PS, the wildtype and variants [C35S] and [C35S,C372S] were transformed into base strain BYt and three strains with disruptions in genes (*PEP4, PRB1*) encoding major yeast vacuolar proteases PrA and PrB (Jones, 1991). Following cultivation for 48 h, samples were collected and TAL levels were determined (Figure 6). TAL titers more than doubled for the protease knockout strains expressing the wildtype 2-PS relative to the base strain, confirming our prior results on the impact of proteases on TAL production (Cardenas and Da Silva, 2014). Increases were also seen for the [C35S] variant, although these were smaller relative to that observed for the wildtype 2-PS. For the [C35S,C372S] variant, titers were higher in all strains (~1.3 g/L), including over 5-fold relative to strain BYt. However, the increases were due to the two 2-PS mutations; in this case, the protease deletions did not further increase TAL titers.

3.6 Fed-batch cultivation of yeast

To determine the TAL levels feasible with fed-batch cultivation, one of the top performing 2-PS variants *in vivo* [C35S,C372S] (Figure 3B) was combined with an engineered yeast strain (BJ5464Δ*pyc2*Δ*nte1*) previously shown to produce high TAL titers (Cardenas and Da Silva, 2014). A supplemented glucose feed (to control the C/N ratio at 35:1) was used, and feed rate was varied to maintain DO levels at 20% and glucose levels low (to prevent repression of the *ADH2* promoter). TAL titer, yield, and glucose concentration were followed for 120 h (Figure 7). This strain achieved a biomass (DCW) concentration of 28 g/L, a yield of 0.18 g/g (38% of theoretical), and a TAL titer of 10.4 g/L. This is a 5-fold increase relative to our previously reported titer for the wildtype 2-PS expressed in the same strain in glucose fed-batch fermentation (Cardenas and Da Silva, 2014).

4. Discussion

4.1 Design and evaluation of 2-PS mutants *in vitro* and *in vivo*

Based on previous studies that identified steric hindrance as a method of defining specificity and selectivity in Type III PKSs, *in vitro* studies were designed for evaluation of 2-PS active site mutations. Based on residues inside the active site location, amino acid changes were selected to create size restriction. Additionally, a C35S mutation was made to reduce oxidation sensitivity due to the observation of its solvent exposure when examining the crystal structure, and mutations to external cysteines have been shown to have negligible effects on *in vitro* enzyme activity (Hayashi et al., 2015). *In vitro* analysis of 2-PS and its mutants was complicated by two factors. First, spontaneous decarboxylation of malonyl CoA to produce acetyl CoA *in situ* made kinetic analysis difficult, and it is unclear whether 2-PS mutants catalyze decarboxylation of malonyl CoA at the same rate as wildtype. Second, oxidation of the active site cysteine, which was observed in the crystallization of 2-PS (Jez et al., 2002), may occur at different rates between the mutant enzymes, which would alter *in vitro* kinetic and enzyme stability assay results. Nevertheless, apparent k_{cat} and K_m

values were calculated to compare 2-PS mutants. [C35S] possessed similar catalytic parameters as wildtype enzyme (Table 1). [C35S,L202F] and [C35S,C372S] possessed the greatest catalytic efficiency, potentially due to tolerance of these enzyme to oxidative inactivation taking place at either the active site or through protein – protein disulfide bond formation. Additionally, constricting the active site *via* the [C35S,L202F] mutation might confer oxidation resistance to the enzyme. Other active site mutants, however, did not increase *in vitro* activity. This could be due to detrimental effects on protein stability conferred by altering the active site.

Interestingly, TAL levels generated from *S. cerevisiae* strains expressing the 2-PS mutants did not always correlate with the *in vitro* kinetics and stability (Figure 2). The importance of [C35S] is highlighted when comparing TAL levels for enzymes [C35A] or [L268F]. The poor *in vitro* activity of [C35A] correlates with TAL production in yeast. Both [C35SL268F] and [L268F] performed poorly *in vitro*. However, [C35SL268F] performed well *in vivo*, whereas [L268F] alone performed poorly. Introduction of a bulky residue *via* I343F severely decreased both *in vivo* and *in vitro* activity. [C35S,I201M] was a poor performer both *in vitro* and in *S. cerevisiae* (Figure 2). The [C35S,T137F] variant did not purify well for kinetics studies and therefore does not have additional parameters available for comparison. From these results, we discovered the effect of several active site residues on enzyme activity and that C35S could be coupled with active site mutations to increase TAL production *in vivo*.

To provide further insight into the effect of these mutations on 2-PS, we investigated the physical properties of the 2-PS mutants *in vitro*. In general, thermal stability decreased when active site mutations were made (Supplementary Figure 4). Since these mutations were designed to constrict the active site, they may destabilize the overall protein fold. Modification of C35 to either alanine or serine had little effect on thermal stability. Further *in vitro* enzyme activity stability assays to measure enzyme “half-life” provided insight into enzyme stability during *in vitro* kinetics experiments (Figure 5). These studies revealed that modification of C35 led to an increase in stability over time, presumably due to elimination of cysteine oxidation or disulfide bond formation. Mutations in the active site also led to greater longevity in solution. This might arise from constriction of the active site, and thus reducing oxidation of the catalytic C169, supported by the increased half-life of [L268F] and [C35S,L202F]. Overall enzyme activity *in vivo* is likely modulated by the oxidation state of surface cysteine residues, and not by protein stability alone. This is illustrated by the contrasting results of the [C35A] and [C35S] mutants. Both showed increased half-lives over WT and similar thermal stabilities, but [C35S] produced significant TAL titer increases in yeast while [C35A] reduced TAL production.

4.2 Altering cysteine residues and host properties leads to increased TAL titers

The observation that cysteine residues would be critical in the stability of 2-PS in yeast was not expected. This study demonstrates the importance of surface cysteine residues and the preferential substitution to a serine, a conservative substitution that retains similar steric and chemical properties. Observation of the crystal structure of 2-PS reveals that C35, C372, and C89 sit at highly solvent exposed positions, whereas all other cysteines are relatively more

buried within the enzyme (Figure 3A). The [C35S] mutation alone improved catalytic efficiency, and was necessary for maintaining 2-PS activity when each other cysteine was mutated (Figure 4). Modification of C372 and C89 led to increased TAL production in yeast, indicating that further elimination of surface cysteines increases enzyme stability *in vivo*. Interestingly, C135 and C195 mutations to serine and alanine, respectively, provided increases in TAL production. These two residues are in close proximity within the protein structure, suggesting that modulation of this potential disulfide bond site allows for greater TAL production *in vivo*. Modification of the buried residue C89 to serine increased TAL production, while modification of C346 to alanine or serine did not increase TAL production, and it is unclear how these modifications might affect activity.

The change in free thiol levels when 2-PS is expressed in yeast underscores the benefits of removing surface cysteine residues to avoid oxidation and formation of undesirable disulfide bonds with 2-PS (Figure 5). It has been reported that oxygen-stress leads to overall poor health of the culture (Koc et al., 2004; Steels et al., 1994), potentially explaining the observation that anaerobic conditions yielded overall lower free thiols than the aerobic system. Proteolytic activity is one means for repairing or recycling damaged protein, including oxidized enzymes (Costa et al., 2007). Previous studies (Cardenas and Da Silva, 2014) and Figure 6 show that the wildtype 2-PS is susceptible to the yeast PrB protease. Employing protease-deficient strains increased TAL titers for the wildtype 2-PS, but does not further improve levels for the [C35S, C372S] variant. The loss in TAL titers when employing cysteine-rich 2-PS variants in the presence of yeast proteases suggests targeted degradation of oxidized 2-PS, supported by the fact that [C35S,C372S] was the most abundant variant when measured by western blot from yeast cultures (Supplementary Figure 5).

Fed-batch culture of the strain BJ5464Δ*pyc2*Δ*nte1* expressing the [C35S,C372S] variant led to the highest TAL production in yeast to date, at over 10 g TAL per liter of culture. The increase in TAL titer and yield relative to prior bioreactor studies was due to both the improved 2-PS enzyme and to the supplemented glucose feed (C/N ratio of 35:1, resulting in extended glucose consumption and a subsequent boost in biomass) (Cardenas, 2015; Cardenas and Da Silva, 2014). Further strains can be designed to suppress the additional biomass formation in favor of TAL production.

5. Conclusions

We have successfully carried out an enzyme engineering approach coupling *in vitro* analysis and *in vivo* biosynthesis to increase the production of the polyketide triacetic acid lactone in *S. cerevisiae*. Through *in vitro* characterization, novel 2-PS variants were constructed to reduce cavity size in the active site and prolong enzyme stability and activity. While there was significant overlap between *in vitro* and *in vivo* results, changes in TAL production were also observed when *in vitro* enzyme kinetic data did not predict *in vivo* behavior. Further investigation revealed the importance of surface-exposed cysteine residues; the C35S mutation was identified as not only improving k_{cat}/K_m of the 2-PS, but also as critical for *in vivo* stability of 2-PS including in variants bearing additional mutations. One successful 2-PS variant had two surface cysteines replaced by serine [C35S,C372S] and increased TAL

titers 2.5-fold relative to wildtype. Using this variant in the engineered BJ5464Δ*pyc2*Δ*nte1* strain led to high-level production of triacetic acid lactone during fed-batch cultivation, reaching 10.4 g/L TAL (38% of theoretical yield). Since [C35S,C372S] exhibited moderate catalytic efficiency, high enzyme stability, and increased TAL titers, it is reasonable to suggest that modification of surface cysteines of enzymes heterologously expressed in yeast will lead to greater *in vivo* performance potentially due to reduced proteolytic degradation. The approach used in this work and the importance of modifying surface-exposed cysteines should prove valuable for the improved *in vivo* biosynthesis of other polyketide products.

Supplementary Material

Refer to Web version on PubMed Central for supplementary material.

Acknowledgements

This research was supported by the National Science Foundation (Grant No. EEC-0813570) through the Engineering Research Center CBiRC (Center for Biorenewable Chemicals), IOS-1516156 and the Howard Hughes Medical Institute.

References

Albers E, Larsson C, Lidén G, Niklasson C, Gustafsson L. 1996 Influence of the nitrogen source on Saccharomyces cerevisiae anaerobic growth and product formation. Appl. Environ. Microbiol 62:3187–3195. [PubMed: 8795209]

Austin MB, Bowman ME, Ferrer J-L, Schröder J, Noel JP. 2004 An aldol switch discovered in stilbene synthases mediates cyclization specificity of type III polyketide synthases. Chem. Biol 11:1179–1194. [PubMed: 15380179]

Austin MB, Noel JP. 2003 The chalcone synthase superfamily of type III polyketide synthases. Nat. Prod. Rep 20:79–110. [PubMed: 12636085]

Cardenas J 2015 Metabolic engineering of Saccharomyces cerevisiae for the high-level synthesis of polyketides. eScholarship. http://escholarship.org/uc/item/5dk5t901.

Cardenas J, Da Silva NA. 2014 Metabolic engineering of Saccharomyces cerevisiae for the production of triacetic acid lactone. Metab. Eng 25:194–203. [PubMed: 25084369]

Cardenas J, Da Silva NA. 2016 Engineering cofactor and transport mechanisms in Saccharomyces cerevisiae for enhanced acetyl-CoA and polyketide biosynthesis. Metab. Eng 36:80–89. [PubMed: 26969250]

Chia M, Schwartz TJ, Shanks BH, Dumesic JA. 2012 Triacetic acid lactone as a potential biorenewable platform chemical. Green Chem. 14:1850–1853.

Costa V, Quintanilha A, Moradas-Ferreira P. 2007 Protein oxidation, repair mechanisms and proteolysis in Saccharomyces cerevisiae. IUBMB Life 59:293–298. [PubMed: 17505968]

Eckermann S, Schröder G, Schmidt J, Strack D, Edrada RA, Helariutta Y, Elomaa P, Kotilainen M, Kilpeläinen I, Proksch P, Teeri TH, Schröder J. 1998 New pathway to polyketides in plants. Nature 396:387–390.

Gietz D, Jean AS, Woods RA, Schiestl RH. 1992 Improved method for high efficiency transformation of intact yeast cells. Nucleic Acids Res. 20:1425–1425. [PubMed: 1561104]

Hayashi Y, Yasugi F, Arai M. 2015 Role of cysteine residues in the structure, stability, and alkane producing activity of cyanobacterial aldehyde deformylating oxygenase. PLoS ONE 10:e0122217. [PubMed: 25837679]

Hertweck C 2009 The biosynthetic logic of polyketide diversity. Angew. Chem. Int. Ed 48:4688–4716.

Hill J, Donald KAIG, Griffiths DE. 1991 DMSO-enhanced whole cell yeast transformation. Nucleic Acids Res. 19:5791–5791. [PubMed: 1945859]

Jez JM, Austin MB, Ferrer J-L, Bowman ME, Schröder J, Noel JP. 2000a Structural control of polyketide formation in plant-specific polyketide synthases. Chem. Biol 7:919–930. [PubMed: 11137815]

Jez JM, Bowman ME, Noel JP. 2001 Structure-guided programming of polyketide chain-length determination in chalcone synthase. Biochemistry (Mosc.) 40:14829–14838.

Jez JM, Bowman ME, Noel JP. 2002 Expanding the biosynthetic repertoire of plant type III polyketide synthases by altering starter molecule specificity. Proc. Natl. Acad. Sci. U. S. A 99:5319–5324. [PubMed: 11959984]

Jez JM, Ferrer J-L, Bowman ME, Dixon RA, Noel JP. 2000b Dissection of malonyl-coenzyme A decarboxylation from polyketide formation in the reaction mechanism of a plant polyketide synthase. Biochemistry (Mosc.) 39:890–902.

Jones EW. 1991 Tackling the protease problem in Saccharomyces cerevisiae. Methods Enzymol. 194:428–453. [PubMed: 2005802]

Kim MI, Kwon SJ, Dordick JS. 2009 In vitro precursor-directed synthesis of polyketide analogues with coenzyme A regeneration for the development of antiangiogenic agents. Org. Lett 11:3806–3809. [PubMed: 19653678]

Koc A, Gasch AP, Rutherford JC, Kim H-Y, Gladyshev VN. 2004 Methionine sulfoxide reductase regulation of yeast lifespan reveals reactive oxygen species-dependent and -independent components of aging. Proc. Natl. Acad. Sci. U. S. A 101:7999–8004. [PubMed: 15141092]

Kraus GA, Wanninayake UK, Bottoms J. 2016 Triacetic acid lactone as a common intermediate for the synthesis of 4-hydroxy-2-pyridones and 4-amino-2-pyrones. Tetrahedron Lett. 57:1293–1295.

Manikandan K, Viruthagiri T, others. 2010 Optimization of C/N ratio of the medium and fermentation conditions of ethanol production from tapioca starch using co–culture of Aspergillus niger and Saccharomyces cerevisiae. Int J Chem Tech Res 2:947–955.

Marienhagen J, Bott M. 2013 Metabolic engineering of microorganisms for the synthesis of plant natural products. J. Biotechnol 163 From Gene to Product:166–178. [PubMed: 22687248]

Nevoigt E 2008 Progress in metabolic engineering of Saccharomyces cerevisiae. Microbiol. Mol. Biol. Rev 72:379–412. [PubMed: 18772282]

Niesen FH, Berglund H, Vedadi M. 2007 The use of differential scanning fluorimetry to detect ligand interactions that promote protein stability. Nat. Protoc 2:2212–2221. [PubMed: 17853878]

Pfeifer BA, Khosla C. 2001 Biosynthesis of polyketides in heterologous hosts. Microbiol. Mol. Biol. Rev 65:106–118. [PubMed: 11238987]

Sambrook JJ, Russell DDW. 2001 Molecular cloning: a laboratory manual. Vol. 2 CSHL Press 778 p.

Saunders LP, Bowman MJ, Mertens JA, Silva NAD, Hector RE. 2015 Triacetic acid lactone production in industrial Saccharomyces yeast strains. J. Ind. Microbiol. Biotechnol 42:711–721. [PubMed: 25682106]

Schwartz TJ, Johnson RL, Cardenas J, Okerlund A, Da Silva NA, Schmidt-Rohr K, Dumesic JA. 2014 Engineering catalyst microenvironments for metal-catalyzed hydrogenation of biologically derived platform chemicals. Angew. Chem. Int. Ed Engl 53:12718–12722. [PubMed: 25196504]

Shanks BH, Keeling PL. 2017 Bioprivileged molecules: creating value from biomass. Green Chem 19:3177–3185.

Shen MWY, Fang F, Sandmeyer S, Da Silva NA. 2012 Development and characterization of a vector set with regulated promoters for systematic metabolic engineering in Saccharomyces cerevisiae. Yeast 29:495–503. [PubMed: 23166051]

Steels EL, Learmonth RP, Watson K. 1994 Stress tolerance and membrane lipid unsaturation in Saccharomyces cerevisiae grown aerobically or anaerobically. Microbiology 140:569–576. [PubMed: 8012580]

Stewart C, Vickery CR, Burkart MD, Noel JP. 2013 Confluence of structural and chemical biology: plant polyketide synthases as biocatalysts for a bio-based future. Curr. Opin. Plant Biol 16:365–372. [PubMed: 23481348]

Tang S-Y, Qian S, Akinterinwa O, Frei CS, Gredell JA, Cirino PC. 2013 Screening for enhanced triacetic acid lactone production by recombinant Escherichia coli expressing a designed triacetic acid lactone reporter. J. Am. Chem. Soc 135:10099–10103. [PubMed: 23786422]

Vickery CR, La Clair JJ, Burkart MD, Noel JP. 2016 Harvesting the biosynthetic machineries that cultivate a variety of indispensable plant natural products. Curr. Opin. Chem. Biol 31:66–73. [PubMed: 26851514]

Wang J, Wang X-H, Liu X, Li J, Shi X-P, Song Y-L, Zeng K-W, Zhang L, Tu P-F, Shi S-P. 2016 Synthesis of unnatural 2-substituted quinolones and 1,3-diketones by a member of type III polyketide synthases from Huperzia serrata. Org. Lett 18:3550–3553. [PubMed: 27399835]

Xie D, Shao Z, Achkar J, Zha W, Frost JW, Zhao H. 2006 Microbial synthesis of triacetic acid lactone. Biotechnol. Bioeng 93:727–736. [PubMed: 16245348]

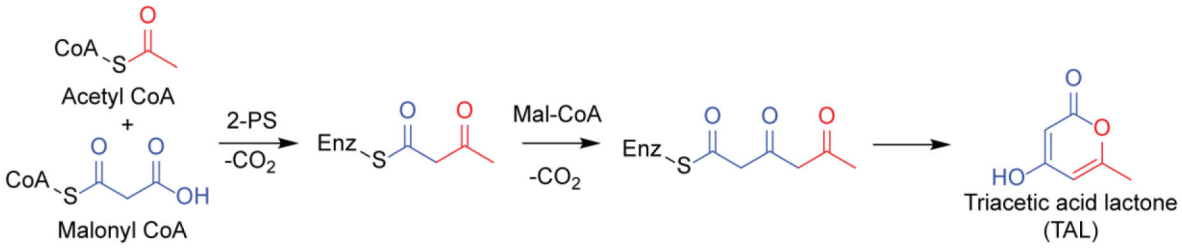

Figure 1:

Decarboxylative condensation and cyclization reaction catalyzed by the type III PKS 2-PS. One molecule of acetyl CoA and two molecules of malonyl CoA are required to form the final product, triacetic acid lactone (TAL). Blue molecules originate from malonyl CoA, and red from acetyl CoA.

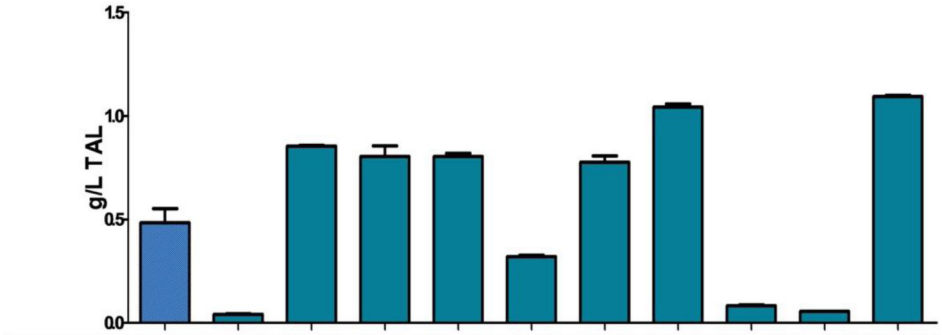

C35 Residue	C	A	S	S		C	S		S	S	S
Position Modified	---	C35	C35	L202		L268	L268		I343	I201	T137
New Residue	---	A	S	M	F	F	M	F	F	M	F

Figure 2:

TAL titers of active site mutants. *S. cerevisiae* strains expressing the 2-PS variants were cultivated for 48 hour and TAL concentration in the broth was assayed by HPLC.

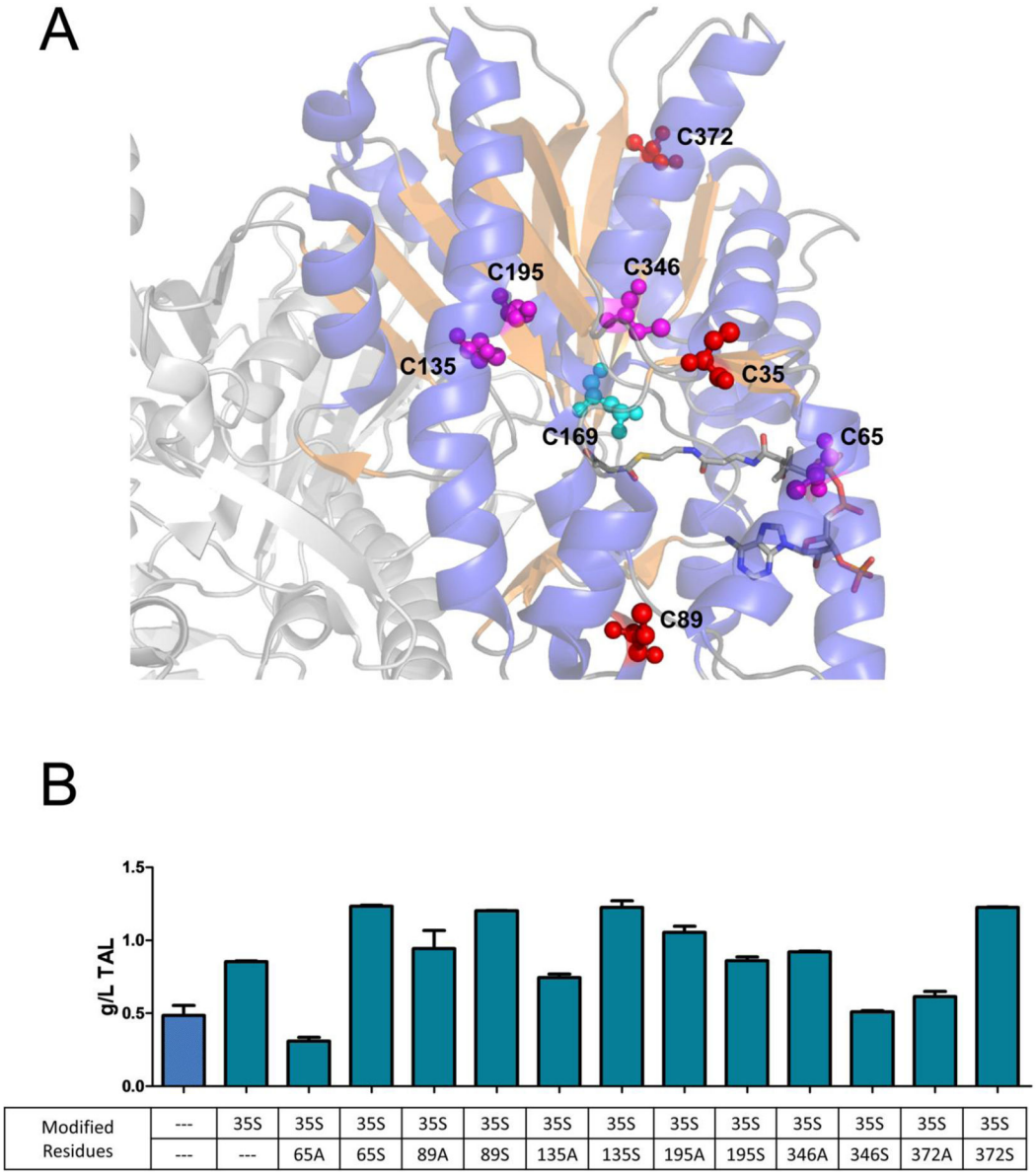

Figure 3:

Effects of modifying cysteine residues. (A) Depiction of 2-PS and the cysteine residues found throughout the protein. C35, C89, and C372 (red) lie on the protein surface. C65, C135, and C195, and C346 (magenta) are buried within the enzyme fold. C169 (teal) is the catalytic cysteine. Malonyl CoA is depicted in stick form. (B) In the presence of the C35S mutation, changes to both surface and buried residues modulates *in vivo* TAL production.

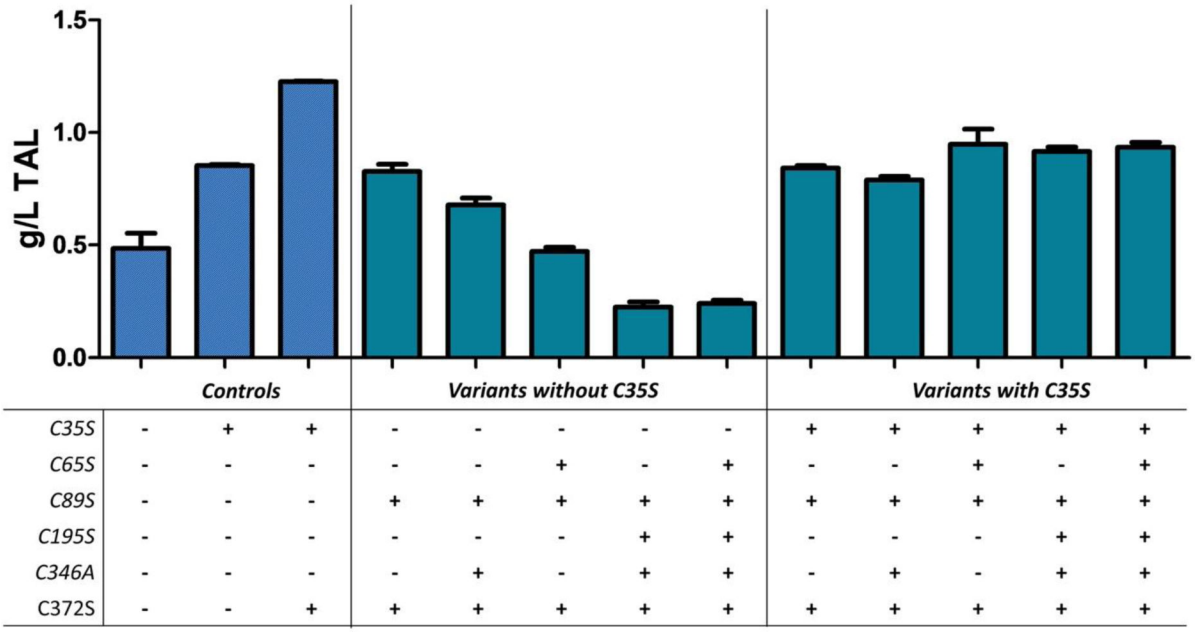

Figure 4:

Combining cysteine mutations. In the absence of C35S, mutation of other cysteine residues in 2-PS do not increase TAL titers relative to C35S alone, although two increase titers relative to the wildtype 2-PS. In the presence of the C35S mutation, variants with altered cysteine residues produce TAL titers comparable to the C35S mutation alone. The exception is C35S, C372S that results in the highest TAL levels.

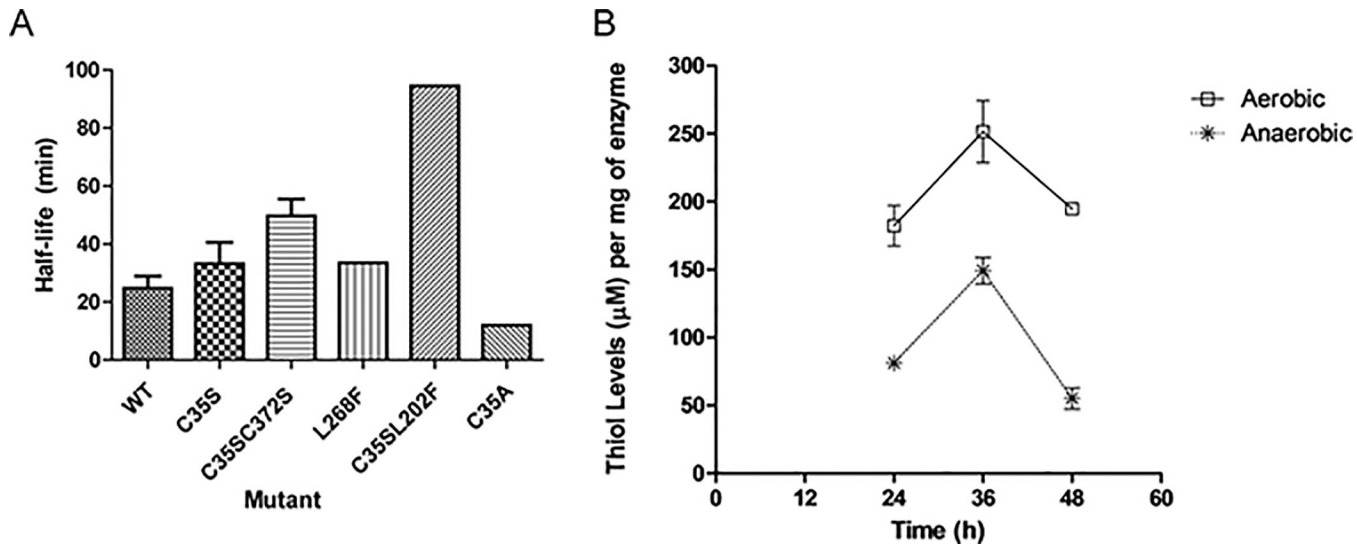

Figure 5:

Potential oxidative effects on 2-PS. (A) The half-life of mutants containing cysteine to serine mutations and mutations that shrink the active site cavity exhibited an increase in half-life over wildtype. (B) Free thiol levels were higher at 36h, indicating potential stress elicited by overexpression of TAL.

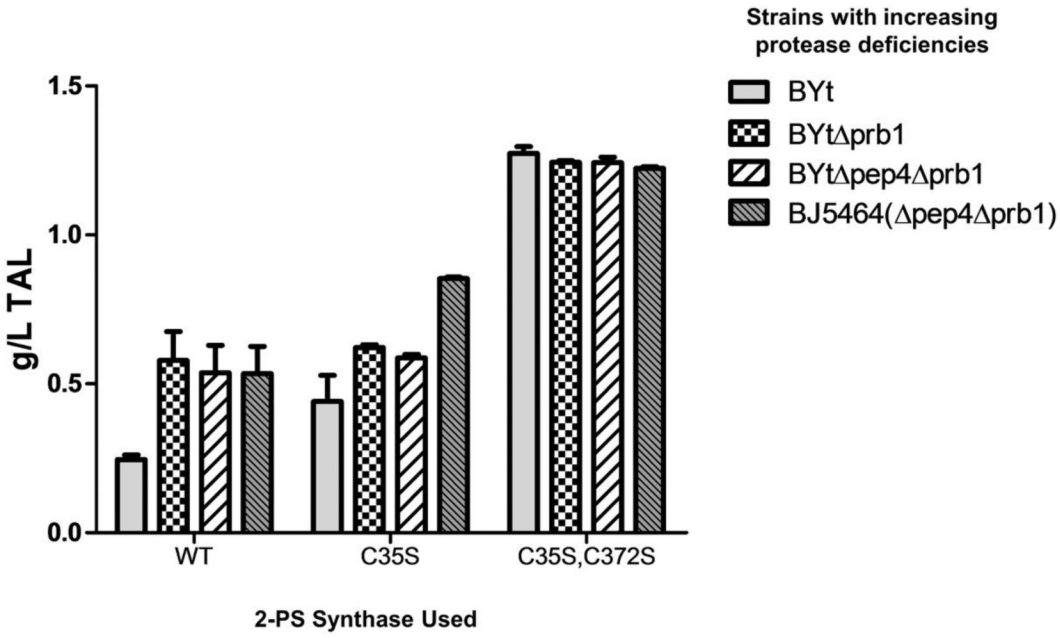

Figure 6:

Native protease deletions affect TAL titers. Increases in TAL levels were observed for strains with *PRB1* deletions expressing the wildtype 2-PS or the C35S variant. No increase was seen for 2-PS variant [C35S,C372S].

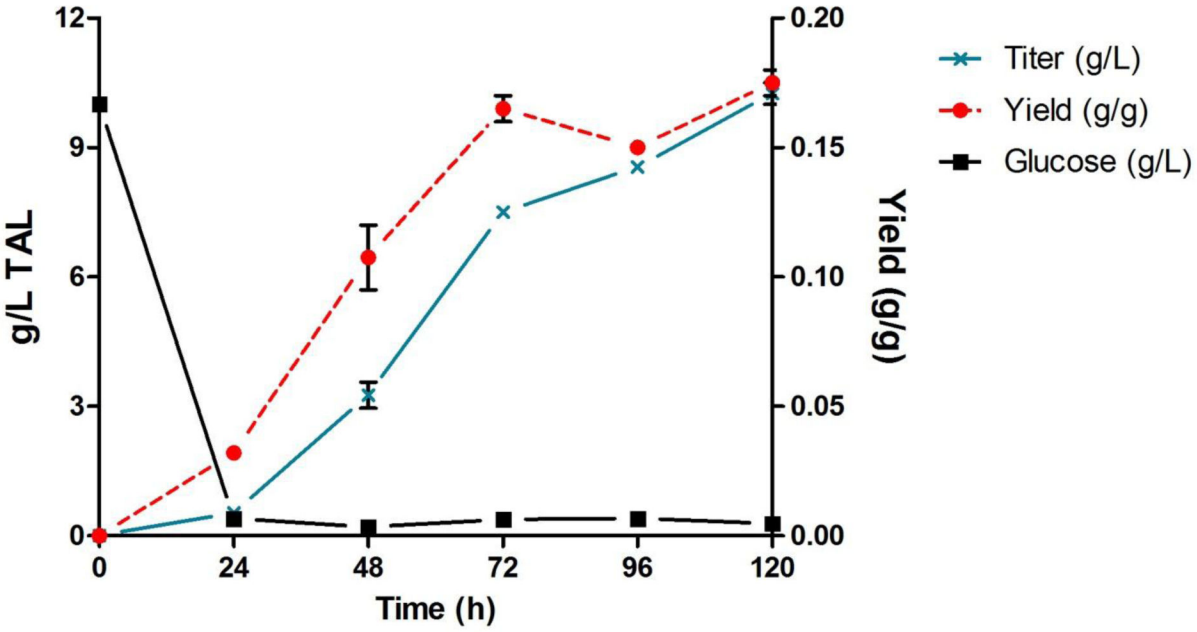

Figure 7:

Fed-batch cultivation of strain BJ5464Δ*pyc2*Δ*nte1* expressing the 2-PS variant C35S,C372S. A supplemented glucose feed was initiated at 12 h. Glucose levels were maintained at a low value to enable high-level transcription of the 2-PS gene from the yeast *ADH2* promoter.

Table 1:

Plasmid constructs utilized in this study. Each 2-PS variant was cloned into pXP842 prior to transformation into yeast strains.

Plasmid	Mutations			Plasmid	Mutations					
WT	N/A			*JC21*	C35S	C65S				
JC1	C35A			*JC22*	C35S	C89A				
JC2	C35S			*JC23*	C35S	C89S				
JC3	L268F			*JC24*	C35S	C135A				
JC4	C35S	L202M		*JC25*	C35S	C135S				
JC5	C35S	L202F		*JC26*	C35S	C195A				
JC6	C35S	L268M		*JC27*	C35S	C195S				
JC7	C35S	L268F		*JC28*	C35S	C346A				
JC8	C35S	I343M		*JC29*	C35S	C346S				
JC9	C35S	I343F		*JC30*	C35S	C372A				
JC10	C35S	M259F		*JC31*	C35S	C372S				
JC11	C35S	T137L		*JC32*	C89S	C372S				
JC12	C35S	T137M		*JC33*	C35S	C89S	C372S			
JC13	C35S	T137F		*JC34*	C89S	C346A	C372S			
JC14	C35S	I201L		*JC35*	C35S	C89S	C346A	C372S		
JC15	C35S	I201M		*JC36*	C65S	C89S	C372S			
JC16	C35S	I201F		*JC37*	C35S	C65S	C89S	C372S		
JC17	C35S	L202F	L268M	*JC38*	C89S	C195S	C346A	C372S		
JC18	C35S	L202F	L268F	*JC39*	C35S	C89S	C195Ss	C346A	C372S	
JC19	C35S	L268M	I343M	*JC40*	C65S	C89S	C346A	C372S		
JC20	C35S	C65A		*JC41*	C35S	C65S	C89S	C195S	C346A	C372S

Table 2:

Kinetics obtained for 2-PS and variants with respect to acetyl CoA.

Mutant	K_m (μM)	k_{cat} (m^{-1})	K_{cat}/K_m ($s^{-1}M^{-1}$)
WT	1.0 ± 0.2	0.54 ± 0.02	8879
C35A	0.3 ± 0.1	0.058 ± 0.003	2891
C35S	0.7 ± 0.1	0.47 ± 0.01	10663
C35SC372S	1.0 ± 0.07	0.76 ± 0.06	12123
C35SL268F	3.0 ± 0.9	0.056 ± 0.004	311
L268F	3.5 ± 1.1	0.42 ± 0.03	2000
C35SL202F	0.16 ± 0.02	0.164 ± 0.004	18265
C35SI201M	0.5 ± 0.1	0.0126 ± 0.001	429
C35SI343F	2.2 ± 0.4	0.11 ± 0.005	818